Neuro-Oncology

*Neuro-Oncology* 18(6), 807–818, 2016
doi:10.1093/neuonc/nov280
Advance Access date 17 November 2015

# $CD4^+$ T effector memory cell dysfunction is associated with the accumulation of granulocytic myeloid-derived suppressor cells in glioblastoma patients

**Daniel Dubinski†‡, Johannes Wölfer†, Martin Hasselblatt, Tilman Schneider-Hohendorf, Ulrich Bogdahn, Walter Stummer, Heinz Wiendl, and Oliver M. Grauer**

*Department of Neurology, University Hospital of Regensburg, Regensburg, Germany (D.D., U.B.); Department of Neurosurgery, University Hospital of Muenster, Muenster, Germany (J.W., W.S.); Institute of Neuropathology, University Hospital of Muenster, Muenster, Germany (M.H.); Department of Neurology, University Hospital of Muenster, Muenster, Germany (T.S.-H., H.W., O.M.G.)*

**Corresponding Author:** Oliver M. Grauer, MD, PhD, Department of Neurology, University of Muenster, Albert-Schweitzer-Campus 1, 48149 Muenster, Germany (oliver.grauer@ukmuenster.de).

†D.D. and J.W. contributed equally to the work.

‡Current address for D.D.: Department of Neurosurgery, University Hospital of Frankfurt, Frankfurt, Germany.

***Background.*** Myeloid-derived suppressor cells (MDSCs) comprise a heterogeneous population of myeloid cells that are significantly expanded in cancer patients and are associated with tumor progression.

***Methods.*** Multicolor flow cytometry was used to study the frequency, phenotype, and function of MDSCs in peripheral blood and freshly resected tumors of 52 participants with primary glioblastoma (GBM).

***Results.*** The frequency of $CD14^{high}CD15^{pos}$ monocytic and $CD14^{low}CD15^{pos}$ granulocytic MDSCs was significantly higher in peripheral blood of GBM participants compared with healthy donors. The majority of granulocytic MDSCs consisted of $CD14^{low}CD15^{high}$ neutrophilic MDSCs with high T-cell suppressive capacities. At the tumor side, we found an increase in $CD14^{high}CD15^{pos}$ monocytic MDSCs and high frequencies of $CD14^{low}CD15^{pos}$ granulocytic MDSCs that displayed an activated phenotype with downregulation of CD16 and upregulation of HLA-DR molecules, which did not inhibit T-cell proliferative responses in vitro. However, a strong association between granulocytic MDSCs and $CD4^+$ effector memory T-cells ($T_{EM}$) within the tumors was detected. Tumor-derived $CD4^+$ $T_{EM}$ expressed high levels of PD-1 when compared with their blood-derived counterparts and were functionally exhausted. The respective ligand, PD-L1, was significantly upregulated on tumor-derived MDSCs, and T-cell co-culture experiments confirmed that glioma-infiltrating MDSCs can induce PD-1 expression on $CD4^+$ $T_{EM.}$

***Conclusions.*** Our findings provide a detailed characterization of different MDSC subsets in GBM patients and indicate that both granulocytic MDSCs in peripheral blood and at the tumor site play a major role in GBM-induced T-cell suppression.

**Keywords:** glioblastoma, myeloid-derived suppressor cell, PD-1, PD-L1, T effector memory cell.

Myeloid-derived suppressor cells (MDSCs) are a heterogeneous population of myeloid cells that are significantly expanded in cancer patients and are associated with tumor progression and poor overall survival.[1] Numerous tumor-derived factors have been described that can induce the accumulation and functional differentiation of MDSCs from hematopoietic progenitor cells in the bone marrow.[2] There is also a large body of evidence that the phenotype and function of MDSCs are largely dependent on the tumor type and specific conditions within the tumor microenvironment.[3,4] MDSCs can suppress T-cell responses by several mechanisms including the depletion of specific amino acids that are essential for T-cell function such as L-arginine and increased production of reactive oxygen species (ROS) such as $H_2O_2$. Arginase I and nitric oxide synthase 2 (NOS2) have been identified as 2 major catabolic enzymes through which MDSCs metabolize L-arginine.[5]

So far, a major difficulty in defining different human MDSC populations is that a specific marker is lacking. MDSCs are usually described by the combination of several myeloid markers such as CD33, CD11b, CD14, and CD15. Therefore, a significant

*Received 12 May 2015; accepted 14 October 2015*

number of different phenotypes have been documented in tumors of different origins.[4,6] Previously, it could be demonstrated that patients with newly diagnosed glioblastoma (GBM) have an increased number of circulating $CD33^+$ $HLA\text{-}DR^-$ MDSCs in their blood that are composed of neutrophilic ($CD15^+$), immature ($CD15^-CD14^-$), and monocytic ($CD14^+$) subsets. Removal of MDSCs from peripheral blood mononuclear cells (PBMCs) with anti-CD33/CD15–coated beads in vitro partially restored T-cell production of IFN-γ after stimulation with anti-CD3/anti-CD28 antibodies. Moreover, significant increases in arginase activity and G-CSF levels were observed in plasma specimens obtained from patients with GBM.[7] Similarly, Sippel et al identified an expanded population of circulating degranulated neutrophils associated with elevated levels of serum arginase I in the blood of GBM patients.[8] The purpose of our study was to compare the frequency, phenotype, and function of MDSCs, both in peripheral blood and freshly resected tumor samples, in a cohort of 52 newly diagnosed GBM participants. Compared with healthy donors, we detected increased frequencies of $CD14^{high}CD15^{pos}$ monocytic and $CD14^{low}CD15^{pos}$ granulocytic MDSCs that were the most prominent, functionally immunosuppressive MDSC subset in the peripheral blood of GBM patients. In addition, we report a strong association between the intratumoral accumulation of $CD14^{low}CD15^{pos}$ granulocytic MDSCs and $CD4^+$ T effector memory ($T_{EM}$) dysfunctions in this patient group.

## Material and Methods

### *Standard Protocol Approvals, Registrations, and Patient Consents*

Participants were recruited at the Departments of Neurology and Neurosurgery at the University Hospital Muenster, Germany, from 2011 until 2014. All experiments were carried out in accordance with the Declaration of Helsinki and were approved by the ethical committee of the University of Muenster Medical School (2010-461-f-S). All participants consented to the scientific use of their biosamples.

### *Preparation of Blood and Tumor Samples*

Blood and freshly resected tumor material were collected from the participants with primary GBM, who had been diagnosed histopathologically according to current WHO criteria. MGMT promotor methylation status was determined as described previously.[9] In addition, blood samples were collected from age- and sex-matched healthy donors. Tumor material was mainly obtained by ultrasonic aspiration using the CUSA Excel system (Integra Radionics Inc.). Ultrasonic aspirates were collected in a sterile suction trap during tumor resection.[10] Tumor fragments were washed extensively to discard blood and suction fluid. Tumor cell suspensions were isolated, as previously described.[11,12] Peripheral blood mononuclear cells (PBMCs) were isolated from EDTA blood by Lymphoprep preparation.

### *Multiparameter Flow Cytometry*

To determine the frequency and phenotype of MDSCs in freshly isolated PBMCs and tumor cell suspensions were stained for 30 minutes at 4°C using a panel of directly labeled monoclonal antibodies (mAbs): CD66b-FITC (fluorescein isothiocyanate), CD124-PE (phycoerythrin), HLADR-ECD (phycoerythrin-Texas Red-X), CD14-PC5.5 (phycoerythrin-cyanin 5.5), CD11b-PC7 (phycoerythrin-cyanin 7), CD33-APC (allophycocyanin), CD19-APC-Alexafluor700, CD16-APC-Alexafluor750, CD15-Pacificblue, and CD45-Krome Orange (all obtained from Beckman Coulter). The viability of $CD45^+$ cells was checked by propidium iodide and was usually >95%. For PD-L1 staining on different MDSC subsets, we used a CD274-APC mAb and the corresponding isotype control (all obtained from eBioscience). For the detection of different T-cell subpopulations, PBMCs and tumor cell suspensions were stained with the following fluorochrome-conjugated mAbs: CD45RA-FITC, CD27-PE, HLADR-ECD, CCR7-PC5.5, CD25-PC7, CD56-APC, CD127-APC, CD3-APC-Alexafluor750, CD4-Krome Orange or CD45RA-FITC, HLADR-PE, CD3-ECD, CD8-PC5.5, CD25-PC7, CD56-APC, CD127-APC-Alexafluor700, CD279 (PD-1)-APC-Alexafluor750, CD27-BV421, and CD4-Krome Orange (obtained from Beckman Coulter or Ebioscience). $CD4^+$ T-cells subsets were defined using the following co-expression of markers: naïve ($T_{NAÏVE}$, $CCR7^+/CD27^+CD45RA^+$), central memory ($T_{CM}$, $CCR7^+/CD27^+CD45RA^-$), effector memory ($T_{EM}$, $CCR7^-/CD27^-CD45RA^-$), terminal differentiated effector memory ($T_{EMRA}$, $CCR7^-/CD27^-CD45RA^+$) T-cells, and regulatory T-cells ($CD4^+CD25^{high}CD127^{low}$). After washing, all samples were analyzed using the Navios flow cytometer and Kaluza 1.2 software (Beckman Coulter.

### *Reactive Oxygen Species and Arginase I Production by MDSC Subsets*

The oxidation-sensitive dye, dichlorodihydrofluorescein diacetate (DCFDA) (Sigma-Aldrich) was used for the measurement of cellular ROS. PBMCs and tumor cell suspensions were washed and incubated with 10 μM DCFDA for 20 minutes at 37 °C. Without washing, cells were then stained with a cocktail of directly labeled mAbs to identify MDSC subsets and were subsequently analyzed by flow cytometry. For arginase I detection, intracellular staining was performed using the eBioscience

**Table 1.** Participant characteristics

| Numbers | Participants = 52 | Controls = 26 |
|---|---|---|
| **Sex** | | |
| Male (*n*) | 33 (63%) | 15 (58%) |
| Female (*n*) | 19 (37%) | 11 (42%) |
| **Median age** | | |
| Years | 63.5 (41–82) | 65.5 (41–79) |
| **Resection status** | | |
| Complete | 25 (48%) | |
| Incomplete | 27 (52%) | |
| **Steroids** | | |
| Received | 34 (65%) | |
| Not received | 18 (35%) | |
| **MGMT status** | | |
| Methylated | 17 (33%) | |
| Unmethylated | 35 (67%) | |

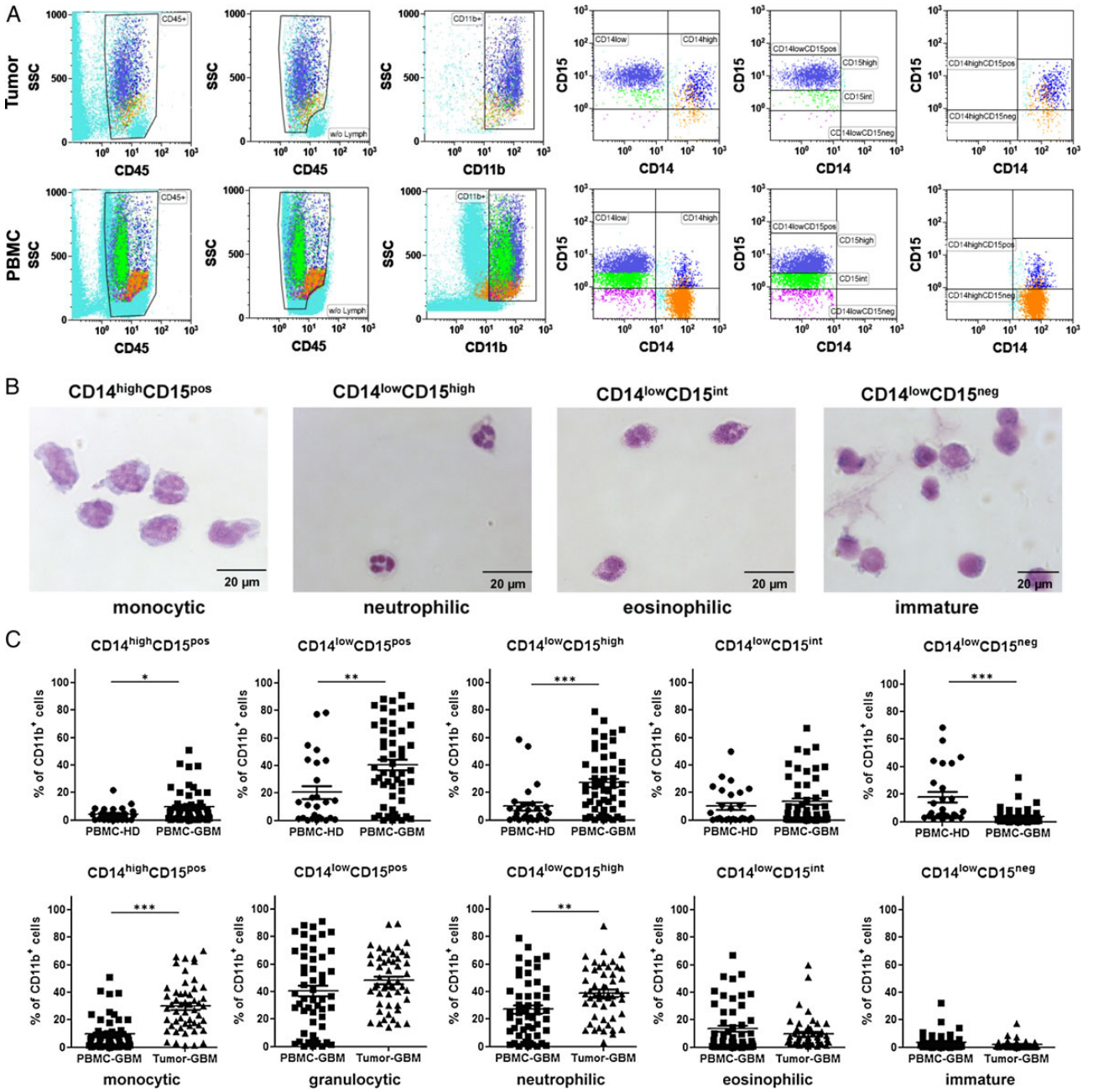


**Fig. 1.** Distribution of different myeloid-derived suppressor cell (MDSC) subsets in peripheral blood and tumor tissue of participants with primary glioblastoma (GBM) (A) Representative dot plots are shown to illustrate the gating strategy for the discrimination of different MDSC subsets. After removal of trash, aggregates, and dead cells by forward/side scatter gating, lymphocytes were excluded from $CD45^{+}$ leukocytes, and cells with high expression of the myeloid marker CD11b were selected to exclude resident microglia or tumor-infiltrating macrophages that usually exhibit a $CD11b^{low}$ expression profile. Cells were then separated into a $CD14^{high}$ and $CD14^{low}$ fraction. Based on the expression of CD15, $CD14^{low}$ cells were further divided into $CD15^{high}$, $CD15^{int}$, or $CD15^{neg}$ cells. Similarly, $CD14^{high}$ cells were split into $CD15^{pos}$ and $CD15^{neg}$ cells. (B) Morphologic characteristics of different MDSC subsets in the peripheral blood of GBM participants. PBMCs were stained with CD45, CD11b, CD14, and CD15, and MDSC subsets were sorted by flow cytometry as depicted in (A). Cytospins and H&E staining were conducted. Representative pictures of different MDSC subsets are shown in (B). $CD14^{high}CD15^{pos}$ cells displayed typical features of monocytes with a lobulated or reniform nucleus (usually eccentrically placed) and a grayish-blue cytoplasm. $CD14^{low}CD15^{high}$ cells revealed the typical morphology of neutrophils with segmented nuclei and pale pink cytoplasm. $CD14^{low}CD15^{int}$ cells displayed features of eosinophils with a classic bilobed nucleus and eosinophilic cytoplasm filled by numerous red granules of uniform size. $CD14^{low}CD15^{neg}$ showed big round nuclei with a small basophilic cytoplasm characteristic for immature myeloid cells. (C) Frequencies of different MDSC subsets within PBMCs and tumor cell suspension of healthy donors (PBMC-HD; $n = 26$) and GBM participants (PBMC-GBM, Tumor-GBM; $n = 52$). *P* values were calculated using the 2-tailed Mann-Whitney test. For detailed statistics, see Supplementary material, Table S1.

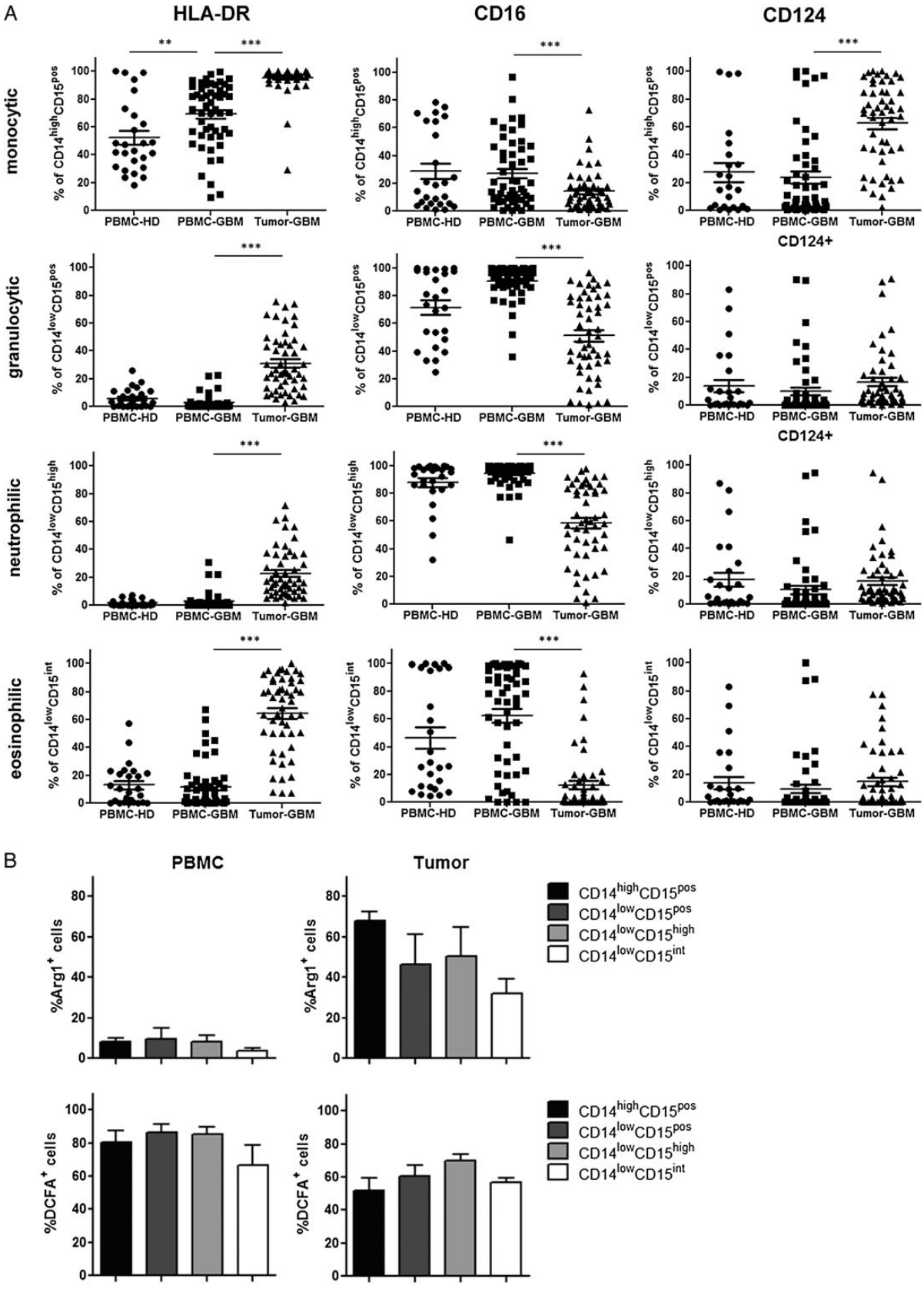
A
HLA-DR
CD16
CD124
monocytic
granulocytic
neutrophilic
eosinophilic
CD124+
PBMC-HD
PBMC-GBM
Tumor-GBM
B
PBMC
Tumor
%Arg1+ cells
%DCFA+ cells
CD14highCD15pos
CD14lowCD15pos
CD14lowCD15high
CD14lowCD15int

fixation/permeabilization procedure including a sheep polyclonal anti-human arginase I-FITC Ab and the appropriate isotype control (R&D Systems).

### *Intracellular INF-γ Secretion*

For intracellular IFN-γ detection, PBMCs, tumor cell suspensions or CSFE-labeled T-cells were stimulated with phorbol 12-myristate 13-acetate (PMA, Sigma-Aldrich, 100 ng/mL) plus ionomycin (Sigma-Aldrich; 1 μg/mL) overnight (16 h) in the presence of Brefeldin A (10 μg/mL). Cells were then stained with T-cell markers, further processed with the Fixation/Permabilization Kit from eBioscience, and labeled with a PE-conjugated IFN-γ mAb (Beckman Coulter).

### *Isolation of MDSC Subsets and T-Cell Assays*

Freshly prepared PBMCs and tumor cell suspensions were labeled with CD45 Krome Orange, CD11b-PC5.5, CD14-FITC, CD15-PB mAbs (Beckman Coulter) and sorted with a FACS Aria III (Becton Dickinson) to isolate different MDSC subsets. Cytospins were prepared from each MDSC subset, and cells were stained with hematoxylin and eosin (H&E) to assess their morphology and purity. Representative pictures were taken under 400x magnification. The viability of MDSCs was assessed using flow cytometry by adding trypan blue to a small fraction of the sorted cells. T-cells were purified using a Pan T-cell isolation kit (MACS, Miltenyi Biotec), resulting in a 95% pure untouched T-cell population as measured by flow cytometry. T-cells were labeled with 2 μM CFSE for 5 minutes (Sigma-Aldrich) in phosphate-buffered saline containing 1% fetal calf serum, washed twice, seeded in a 96-well round-bottom plate coated with coated human anti-CD3 (Okt3) mAb (10 μg/mL, eBioscience) at $5 \times 10^4$/well, and co-cultured with MDSC subsets at a cell ratio of 2:1 for 5 days at 37°C in complete medium in the presence of 100 U/mL IL-2 (Peprotech). T-cell proliferation was monitored by flow cytometric analysis of CFSE fluorescence intensity after staining with PC5.5-labeled anti-CD3 mAb. T-cells in culture medium alone were used as background controls. Co-cultures were conducted in triplicates. For PD-1 induction, freshly prepared tumor-derived MDSCs were co-cultured with untouched T-cells purified from autologous PBMCs at a cell ratio of 1:1. Unstimulated T-cells or T-cells stimulated with 1 μg/mL human anti-CD3 and 2 μg/mL human anti-CD28 mAbs (eBioscience) were used as controls. Cells were harvested after 2 days of culture and analyzed by multicolor flow cytometry for the expression of PD-1 on $CD4^+$ T-cell subsets.

### *Statistical Analysis*

The data were analyzed with the Kolmogorov–Smirnov procedure to test for normal distribution. Because not all groups showed a normal distribution, the following nonparametric tests were used. The 2-tailed Mann-Whitney test was used to test for significant differences between 2 groups, and the Kruskal–Wallis test with post hoc Dunn multiple comparison analysis was applied to test for significant differences between 3 or more groups. For correlation analysis, we used the Spearman rank test. Values of $P < .05$ were considered to be significant. Error bars represented the standard error of the mean. GraphPad Prism 5.0 (GraphPad Software Inc.) was used for statistical analyses.

## Results

### *Phenotype, Morphology, and Frequency of Different MDSC Subsets in Peripheral Blood and Tumor Tissue of Primary Glioblastoma Patients*

To analyze different MDSC subsets in blood and tumor tissue of the primary GBM participants, we conducted multicolor flow cytometry as described in the Materials & Methods section. In total, 52 GBM participants (33 male and 19 female) with a median age of 63.5 years (range: 41–82 y) were included in the study (see Table 1). MDSC subsets were distinguished based on the expression of CD45, CD11b, CD14, and CD15. As has been previously demonstrated for melanoma patients,[13] $CD45^+$ leukocytes with high expression of the myeloid marker CD11b were separated into $CD14^{high}$ and $CD14^{low}$ expressing cells. $CD14^{high}$ cells were split into $CD15^{pos}$ and $CD15^{neg}$ cells, whereas $CD14^{low}$ cells were divided into $CD15^{high}$, $CD15^{int}$, or $CD15^{neg}$ cells (Fig. 1A). Subsequently, MDSC subsets were isolated using a cell sorter and stained with H&E after preparation of cytospin slides. As depicted in Fig. 1B, we confirmed that these phenotypically classified MDSC subsets matched the morphology of common myeloid cells in peripheral blood. $CD14^{high}CD15^{pos}$ cells displayed typical features of monocytes, whereas $CD14^{low}CD15^{high}$ cells revealed the typical morphology of neutrophils. $CD14^{low}CD15^{int}$ cells could be identified as eosinophils, and $CD14^{low}CD15^{neg}$ showed characteristics of immature myeloid cells. Next, we calculated the relative frequency of different MDSC subsets within PBMCs and tumor cell suspensions of GBM participants and healthy donors. Figure 1C shows that GBM participants had an increased percentage of $CD14^{high}CD15^{pos}$ monocytic MDSCs (mean: 9.7% vs 4.3%, $P = .0435$) and granulocytic $CD14^{low}CD15^{pos}$ MDSCs (mean: 40.6% vs 20.6%, $P = .0023$), mainly neutrophilic $CD14^{low}CD15^{high}$ MDSCs (mean: 27.1% vs 10.1%, $P = .0002$) in their blood when compared with age- and sex-matched healthy donors, whereas the percentage of immature $CD14^{low}CD15^{neg}$ MDSCs (mean: 3.9% vs 18.1%, $P < .0001$) was significantly reduced. Moreover, we could detect a significant increase in the frequency of both $CD14^{high}CD15^{pos}$ monocytic (mean: 29.9% vs 9.7%, $P < .0001$) and $CD14^{low}CD15^{high}$ neutrophilic (mean: 38.8% vs 27.1%, $P = .0029$) MDSCs at the

**Fig. 2.** Further phenotypic characterization of different myeloid-derived suppressor cell (MDSC) subsets in peripheral blood and tumor tissue of participants with primary glioblastoma (GBM). (A) The expression of HLA-DR, CD16, and CD124 on different MDSC subsets was evaluated by flow cytometry. The frequencies of HLA-DR, CD16, and CD124-positive MDSCs within peripheral blood mononuclear cells (PBMCs) and tumor cell suspensions of healthy donors ($n = 26$) and GBM participants ($n = 52$) are shown. Asterisks denote significant $P$ values: * $P < .05$; ** $P < .01$; *** $P < .0001$. (B) Arginase I and reactive oxygen species (ROS) production by different MDSC subsets were determined by flow cytometry. The frequencies of arginase I and ROS-positive MDSCs from 5 GBM participants are presented.

tumor site. CD14$^{low}$CD15$^{pos}$ granulocytic MDSCs represented the most prominent MDSC subset inside the tumor, with almost 50% of CD45$^{+}$CD11b$^{high}$ cells. (For detailed statistics, see Supplementary material, Table S1).

### *MDSCs From Peripheral Blood and Tumor Tissue are Phenotypically Different in Patients with Primary Glioblastoma*

To further characterize these cell populations, we assessed the expression of additional myeloid markers on different MDSC subsets. Flow cytometric analysis showed that HLA-DR (MHC class II molecule) was significantly upregulated on monocytic CD14$^{high}$CD15$^{pos}$ MDSCs in the blood of GBM participants when compared with healthy donors, whereas granulocytic CD14$^{low}$CD15$^{pos}$ MDSCs remained negative for HLA-DR. In contrast, HLA-DR was significantly upregulated on both tumor-derived monocytic and granulocytic MDSCs, mainly on CD14$^{low}$CD15$^{int}$ eosinophilic MDSCs. Moreover, we could find significant downregulation of CD16 (FcγRIII) on tumor-derived monocytic and granulocytic MDSCs when compared with blood-derived MDSCs. Remarkably, upregulation of CD124 (IL-4Rα chain) was mainly restricted to tumor-derived CD14$^{high}$CD15$^{pos}$ monocytic MDSCs (Fig. 2A). In addition, we determined the ability of freshly prepared MDSC subsets to express arginase I and to produce ROS. As depicted in Fig. 2B, arginase I was strongly upregulated in tumor-derived MDSCs, predominantly in monocytic MDSCs, whereas only a minor fraction of MDSCs in the blood expressed arginase I. In contrast, ROS could be produced by both MDSC subsets (Fig. 2B).

### *Blood-derived Neutrophilic MDSCs Can Inhibit the Proliferation of Autologous T-Cells in Vitro*

We next evaluated the ability of different MDSC subsets for their T-cell immunosuppressive capacities. Therefore, MDSCs were sorted and analyzed in a standard autologous nonspecific T-cell proliferation assay. As shown in Fig. 3A, neutrophilic and, to a lesser extent, eosinophilic blood-derived MDSCs reduced T-cell proliferation, whereas tumor-derived MDSCs did not show T-cell suppressive capacities in vitro. Additional analysis confirmed that neutrophilic blood-derived MDSCs not only

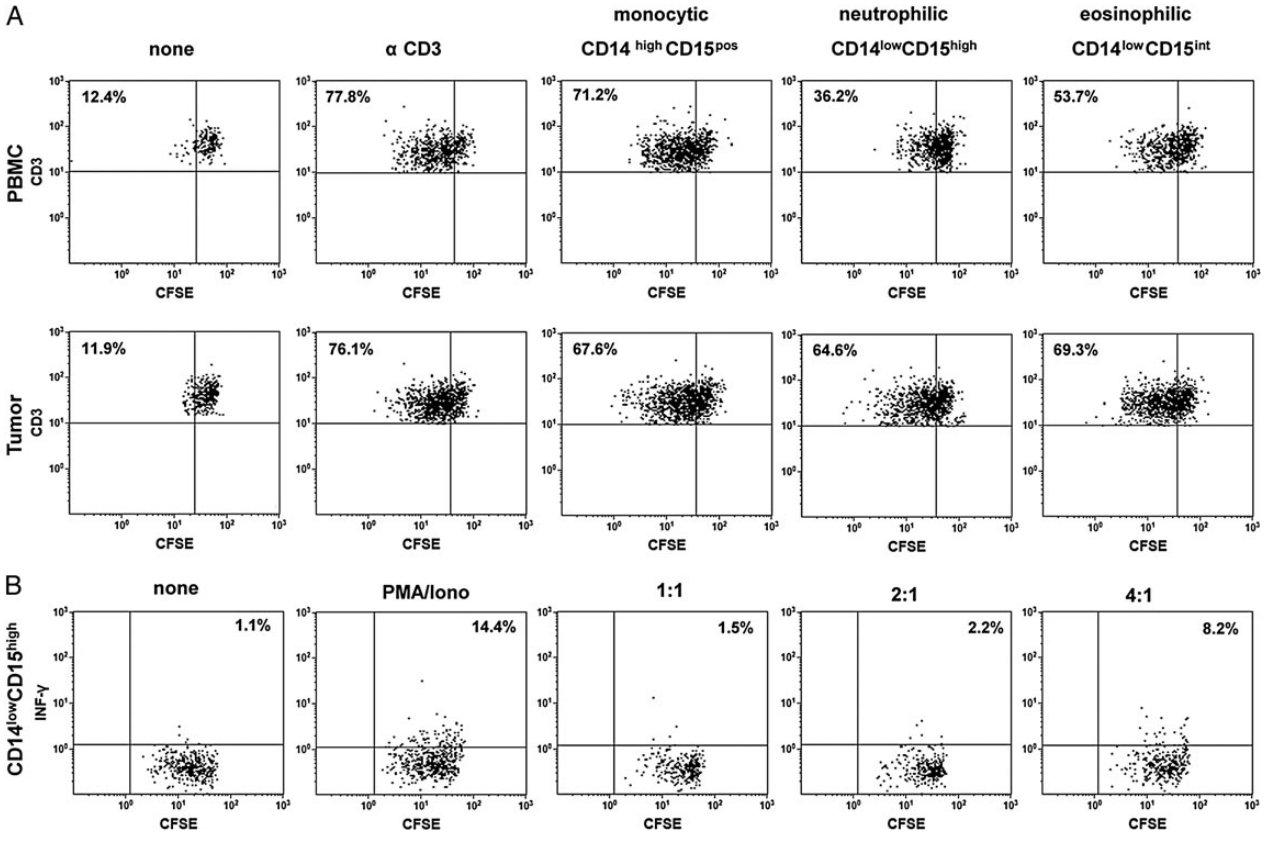


**Fig. 3.** Suppressive capacity of different myeloid-derived suppressor cell (MDSC) subsets from partiipants with primary glioblastoma. Peripheral blood mononuclear cells (PBMCs) and tumor cell suspensions were stained with CD45, CD11b, CD14, and CD15, and different MDSC subsets were sorted, seeded into anti-CD3–coated plates and co-cultured with CFSE-labeled autologous T-cells at a T-cell-to-MDSC ratio of 2:1 in the presence of IL-2. Five days later, T-cell proliferation was assessed by flow cytometry. (A) Representative dot plots of T-cell proliferation after addition of CD14$^{high}$CD15$^{pos}$ monocytic, CD14$^{low}$CD15$^{high}$ neutrophilic, and CD14$^{low}$CD15$^{int}$ MDSCs from the same participant are shown. The percentage values represent the fraction of proliferating CSFE-labeled T-cells. (B) Representative dot plots of T-cell proliferation and intracellular INF-γ secretion after addition of CD14$^{low}$CD15$^{high}$ neutrophilic MDSCs to CFSE-labeled autologous T-cells at different T-cell -to- MDSC ratios (1:1–4:1) and PMA/ionomycin stimulation. The percentage values represent the fraction of INF-γ secreting CSFE-labeled T-cells. Data are representative of 3 independent experiments done.

inhibited T-cell proliferation but also reduced INF-γ secretion by anti-CD3 stimulated autologous T-cells (Fig. 3B). The same results were found when using blood-derived $CD14^{low}CD15^{pos}$ granulocytic MDSCs as total cell population (data not shown).

### *The Frequency of Tumor-derived Granulocytic MDSCs Correlates With the Frequency of Tumor-infiltrating PD-1 Expressing $CD4^+$ T Effector Memory Cells*

Because tumor-derived MDSCs displayed an activated phenotype with downregulation of CD16 and upregulation of HLA-DR, we next investigated the relationship between the frequency of different MDSC and CD4+ T-cell subsets inside the tumor. As shown in Fig. 4A, CD4+ $T_{EM}$ was shown to be the most dominant T-cell subtype infiltrating GBMs, which was about 30% of $CD4^+$ T-cells. Correlation analysis revealed that the frequency of granulocytic MDSCs was positively associated with the frequency of $CD4^+$ $T_{EM}$ at the tumor site (Fig. 4B). Significant correlations between other MDSC subsets and tumor-infiltrating $CD4^+$ T-cell subpopulations, including regulatory T-cells (Tregs), could not be found (data not shown). Based on these results, we looked carefully for phenotypical and

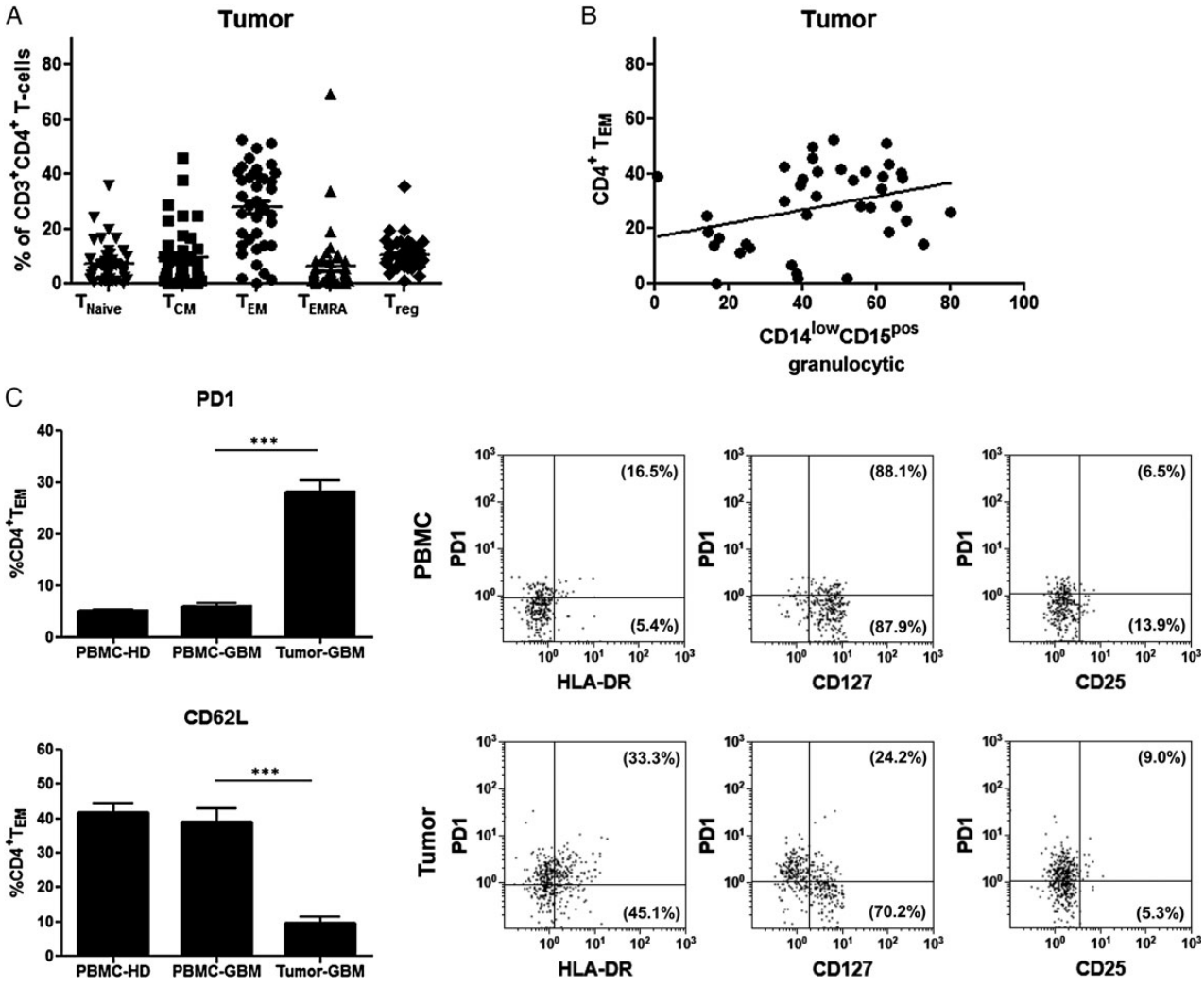


**Fig. 4.** (A) Distribution of intratumoral $CD4^+$ T-cell subpopulations. Lymphocytes selected by side scatter versus forward scatter were displayed in a $CD3^+$ versus $CD4^+$ plot, and T-cell subsets were identified by the following co-expression of CD45RA and CCR7. The proportion of $CD4^+$ T-cell subsets was as follows: $T_{Naïve}$ ($CCR7^+/CD45RA^+$, mean: 7.5 ± 7.5) ; $T_{CM}$ ($CCR7^+/CD45RA^-$, mean: 9.4% ± 10.9); $T_{EM}$ ($CCR7^-/CD45RA^-$, mean: 27.9% ± 14.9); $T_{EMRA}$ ($CCR7^-/CD45RA^+$; mean: 6.5% ± 12.1); Treg ($CD4^+CD25^{high}CD127^{low}$, mean: 10.4 ± 5.9). (B) Correlation of $CD4^+$ $T_{EM}$ and $CD14^{low}CD15^{pos}$ granulocytic myeloid-derived suppressor cell (MDSCs) within primary glioblastoma (GBM) tissue. The frequencies of $CD14^{low}CD15^{pos}$ granulocytic MDSCs and $CD4^+$ $T_{EM}$ at the tumor site from 39 GBM participants were determined by flow cytometry, and correlations between both populations were assessed using Spearman's test ($r = 0.3362$, $P = .0364$). (C) Phenotypic comparison of $CD4^+$ $T_{EM}$ in peripheral blood and tumor tissue of participants with primary GBM. The percentages of PD-1 and CD62L expressing $CD4^+$ $T_{EM}$ within PBMCs and tumor cell suspensions of GBM participants ($n = 29$) and healthy donors ($n = 29$) are shown (mean ± SEM). Asterisks denote significant $P$ values: ***$P < .0001$. In addition, representative dot plots with co-expression of PD-1 and HLA-DR, CD127 or CD25 are depicted. The percentage values represent the fraction of PD-$1^+$ or PD-$1^-$ $CD4^+$ $T_{EM}$ that expressed HLA-DR, CD127 or CD25.

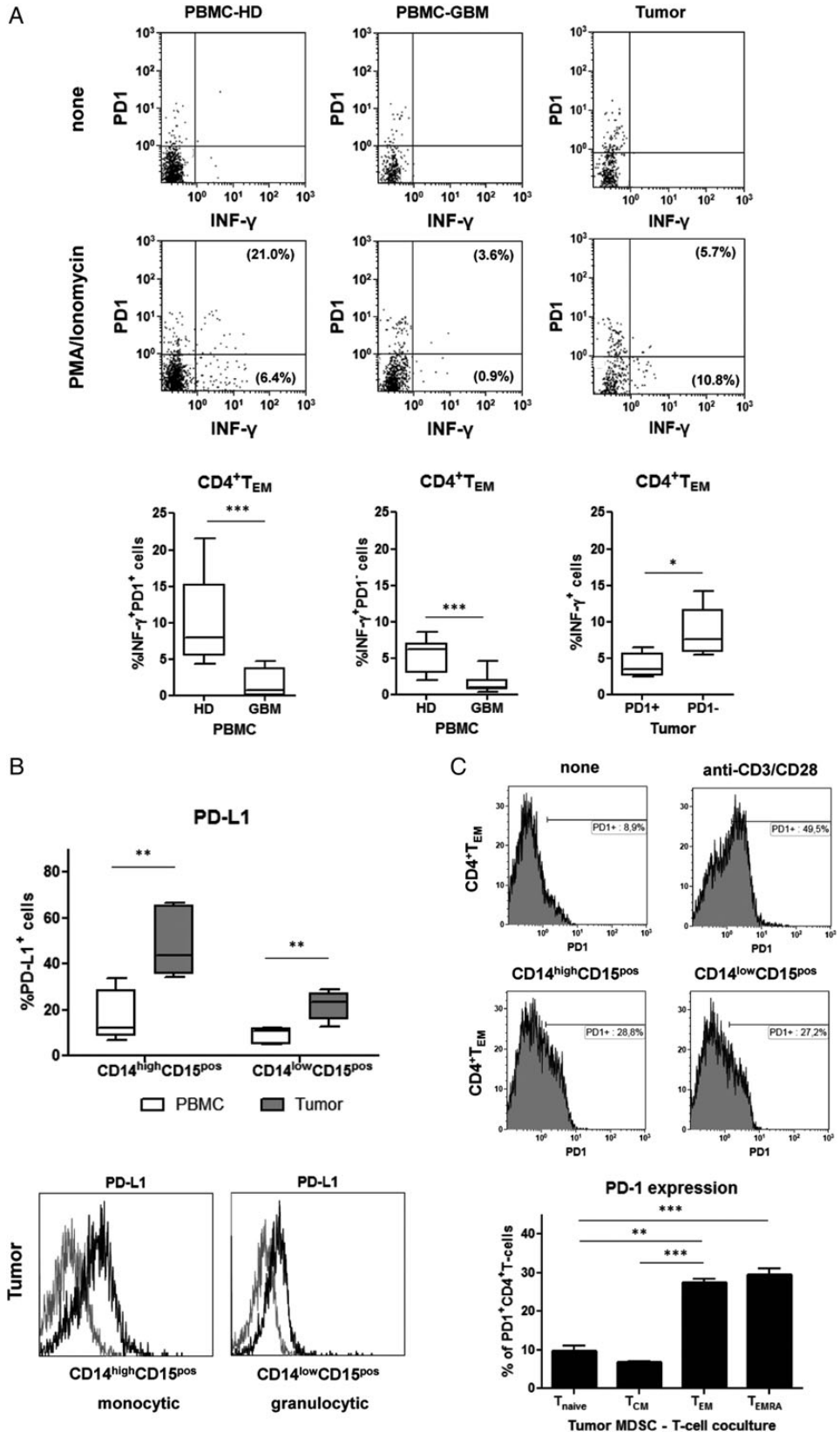
A
PBMC-HD
PBMC-GBM
Tumor
none
PMA/Ionomycin
PD1
INF-γ
(21.0%)
(6.4%)
(3.6%)
(0.9%)
(5.7%)
(10.8%)
CD4+TEM
%INF-γ+PD1+ cells
%INF-γ+PD1- cells
%INF-γ+ cells
HD
GBM
PBMC
PD1+
PD1-
Tumor
B
PD-L1
%PD-L1+ cells
CD14highCD15pos
CD14lowCD15pos
PBMC
Tumor
monocytic
granulocytic
C
none
anti-CD3/CD28
PD1+ : 8,9%
PD1+ : 49,5%
PD1+ : 28,8%
PD1+ : 27,2%
PD-1 expression
% of PD1+CD4+T-cells
Tnaive
TCM
TEM
TEMRA
Tumor MDSC - T-cell coculture

functional differences between blood-derived and tumor-infiltrating $CD4^+$ $T_{EM}$ with regard to the expression of CD279 (PD-1), CD62L (L-selectin), HLA-DR, CD25 (IL-2Rα subunit), and CD127 (IL-7Rα subunit). As demonstrated in Fig. 4C, the frequency and expression level of PD-1 was significantly higher on tumor-infiltrating $T_{EM}$ when compared with blood-derived $T_{EM}$ from GBM participants or healthy donors. In contrast, CD62L expression was significantly downregulated on tumor-infiltrating $T_{EM}$. We also found that a substantial portion of PD-$1^+$ $T_{EM}$ expressed HLA-DR. The majority of PD-$1^+$ $T_{EM}$ was negative for CD127 (IL-7Rα chain), whereas PD-$1^-$ $T_{EM}$ expressed CD127. Irrespective of PD-1 expression, both blood-derived and tumor-infiltrating $T_{EM}$ lacked or showed only low levels of CD25 expression. In contrast, blood-derived $T_{EM}$ did not show upregulation of HLA-DR and were strongly positive for CD127.

### *PD-1 Expressing $CD4^+$ TEM Within Glioblastomas Are Functionally Exhausted and Can Be Induced by PD-L1 Expressing Tumor-derived MDSCs*

Since tumor-infiltrating $T_{EM}$ displayed a marker profile typically associated with T-cell exhaustion, we next determined whether they were impaired in their effector function. Therefore, freshly prepared tumor cell suspensions were stimulated with PMA and ionomycin and assessed for intracellular production of INF-γ. As demonstrated in Fig. 5A, PMA/ionomycin activation resulted in the production of INF-γ by blood-derived PD-$1^+$ and PD-$1^-$ $T_{EM}$ from healthy donors. In contrast, blood-derived $PD1^+$ and $PD1^-$ $T_{EM}$ from GBM participants did not produce relevant amounts of INF-γ after PMA/ionomycin activation. At the tumor site, INF-γ production could be detected mainly in PD-$1^-$ $T_{EM}$ when compared with PD-$1^+$ TEM. Similar results were measured in blood and tumors from multiple patients. The frequency of INF-γ producers was not different between blood-derived and tumor-infiltrating PD-$1^+$ $T_{EM}$ from GBM participants but did differ significantly between blood-derived PD-$1^+$ $T_{EM}$ from healthy donors and tumor-infiltrating PD-$1^+$ $T_{EM}$ from GBM participants ($P = .0026$). In general, lower levels of INF-γ expression were found in $T_{EM}$ from GBM participants when compared with healthy donors. To link CD4+ $T_{EM}$ exhaustion with the presence of granulocytic MDSCs at the tumor site, we further investigated whether MDSCs obtained from peripheral blood and tumor tissue express PD-1 ligand (CD274, PD-L1). We detected a significant increase in the proportion of PD-L1 expressing MDSCs within the tumor when compared with their counterparts in peripheral blood (with higher frequencies in the monocytic MDSC population). Figure 5B shows that both monocytic and granulocytic MDSCs markedly upregulate PD-L1 inside the tumor. Finally, co-culture experiments with purified autologous T-cells showed that tumor-derived MDSCs can induce PD-1 expression on $CD4^+$ $T_{EM}$. Moreover, this effect was seen preferentially on the $CD4^+$ effector memory cell population but not on naïve or central memory $CD4^+$ T-cells (Fig. 5C). These data further point toward a potential role of tumor-derived MDSCs in driving $CD4^+$ $T_{EM}$ exhaustion.

## Discussion

Our study provides a detailed characterization of the frequency, phenotype, and suppressive function of distinct MDSC subsets in peripheral blood and tumor tissue of a large cohort of participants with primary GBM. In peripheral blood, we found that both the proportion of $CD14^{high}CD15^{pos}$ monocytic and $CD14^{low}CD15^{pos}$ granulocytic MDSCs was significantly higher compared with healthy controls. The majority of granulocytic MDSCs consisted of $CD14^{low}CD15^{pos}$ neutrophilic MDSCs. These results confirm previous data from Sippel et al, who reported an expanded population of neutrophils in the blood of GBM patients[8] and are consistent with very recent observations made by Gielen et al, who also detected an increase of monocytic and polymorphonuclear MDSCs.[13] At the tumor side, we found a large proportion of $CD14^{low}CD15^{pos}$ granulocytic MDSCs that consisted mainly of neutrophilic $CD14^{low}CD15^{high}$ MDSCs but also an increased frequency of $CD14^{high}CD15^{pos}$ monocytic MDSCs. These findings are supported by recently published data from Raychaudhuri et al, who observed a predominance of granulocytic ($CD15^+CD14^-$) over monocytic ($CD15^-CD14^+$) MDSCs in tumor specimens of GBM patients, although the percentages they reported were quite different from ours.[14] In contrast, Gielen et al almost exclusively detected $CD15^+CD14^-$ MDSCs within GBM tissue located both in viable and necrotic tumor areas.[13] These discrepancies can be explained by the lower number of patients analyzed, different

**Fig. 5.** (A) Freshly isolated peripheral blood mononuclear cells (PBMCs) and tumor cell suspensions from healthy donors ($n = 6$) and glioblastoma (GBM) participants ($n = 6$) were stimulated with PMA/ionomycin overnight, stained with appropriate mAbs, and analyzed for intracellular INF-γ production. Cells were gated on $CD4^+$ $T_{EM}$, and INF-γ secretion was calculated for PD-$1^+$ and PD-$1^-$ $CD4^+$ $T_{EM}$. Representative dot plots with co-expression of PD-1 and INF-γ of $CD4^+$ $T_{EM}$ from a healthy donor (HD) and a GBM participant as well as boxplots (Min to Max) from all patients analyzed are shown. The percentage values represent the fraction of PD-$1^+$ or PD-$1^-$ $CD4^+$ $T_{EM}$ that produced INF-γ (PBMCs: % INF-$\gamma^+$ PD-$1^+$ $CD4^+$ $T_{EM}$ HD vs GBM, $P < .0001$; % INF-$\gamma^+$ PD-$1^+$ $CD4^+$ $T_{EM}$ HD vs GBM, $P = .0004$; tumor: % INF-$\gamma^+$ PD-$1^+$ vs % INF-$\gamma^+$ PD-$1^-$ $CD4^+$ $T_{EM}$, $P = .0152$). (B) PD-L1 expression on different MDSC subsets in patients with primary GBM. Myeloid-derived suppressor cells (MDSCs) obtained from peripheral blood and tumor tissue ($n = 5$) were stained with appropriate mAbs and analyzed by flow cytometry (boxplots at the top). The percentage of PD-L1 expressing MDSCs (mean ± SEM) and representative histograms of the PD-L1 expression levels on tumor-derived MDSC subsets (grey line: isotype control, black line: PD-L1) are shown at the bottom of the figure ($CD14^{high}CD15^{pos}$ or $CD14^{low}CD15^{pos}$: peripheral blood mononuclear cells vs tumor: $P = .0079$). (C) PD-1 upregulation on $CD4^+$ T-cells after co-culture with tumor-derived MDSC subsets. Tumor-derived MDSCs were sorted and co-cultured with untouched T-cells purified from autologous PBMCs for 2 days. Unstimulated T-cells and anti-CD3/28– stimulated T-cells were used as controls. Cells were harvested, stained with appropriate mAbs, and analyzed by flow cytometry. Representative dot histograms of PD-1 expression on $CD4^+$ $T_{EM}$ are shown at the top. Moreover, PD-1 upregulation (mean ± SEM) of different $CD4^+$ T-cell subsets after co-culture with tumor-derived MDSCs ($n = 4$ GBM patients) are shown at the bottom of the figure. Asterisks denote significant $P$ values: *** $P < .0001$, ** $P < .01$.

techniques for preparing tumor cell suspensions, and different gating strategies for identifying MDSCs subsets. We also checked whether the MGMT methylation status of the tumor or the use of corticosteroids influenced the frequency of MDSC subsets in blood and tumors but could not detect significant differences between tumors with unmethylated or methylated MGMT status or steroid users and non-users in our large participant cohort (Supplementary material, Figs S1 and S2).

Once infiltrating into GBM tissue, MDSCs are strongly modified by the tumor microenvironment. We detected that both granulocytic and monocytic MDSCs showed an activated phenotype with downregulation of CD16 and upregulation of HLA-DR, which was most prominent in monocytic MDSCs. While eosinophilic MDSCs also revealed strong upregulation of HLA-DR, neutrophilic MDSCs displayed a diverse HLA-DR expression pattern. Further subanalysis showed that HLA-DR$^{low/-}$ neutrophilic MDSCs were CD16 positive, expressed CD124, and were arginase I positive, whereas HLA-DR positive neutrophilic MDSCs were CD16 negative, did not express CD124, and were arginase I negative (data not shown). This also suggests that there is an enormous plasticity within the granulocytic fraction of MDSCs within GBMs. Monocytic MDSCs were strongly positive for CD124 and arginase I, in contrast to their counterparts in peripheral blood. These cells also strongly expressed CD206 and the GM-CSF receptor (data not shown) and thus might correspond to the population of previously described tumor-associated macrophages displaying an M2 phenotype.[15] Recently, Kohanbash et al showed that CD124 mediates the IL-13-induced production of arginase within bone marrow-derived myeloid cells, which suppressed T-cell proliferation in an IL-4Rα-dependent manner.[16] They also identified a fraction of CD33$^+$CD14$^+$HLADR$^-$ cells within GBMs that expressed CD124 and suppressed the proliferation of autologous CD8$^+$ T-cells.

Our study also adds insight into the contribution of different MDSC subsets to the inhibition of T-cell activity in peripheral blood and tumor tissue. We observed that mainly freshly isolated blood-derived neutrophilic and (less effectively) eosinophilic MDSCs, but not monocytic MDSCs, were able to suppress autologous nonspecific T-cell proliferation and IFN-γ secretion in vitro. This is in line with previous reports demonstrating that peripheral cellular immunosuppression in GBM patients is mediated by degranulated neutrophils or CD33$^+$HLA$^-$DR$^-$CD15$^+$ cells.[7,8] Altogether, these results clearly demonstrate that granulocytic MDSCs are the functionally immunosuppressive subset in the blood of GBM participants. In contrast, freshly isolated tumor-derived MDSCs did not show T-cell inhibitory capacities in our standard T-cell suppression assay. Similar observations have been made by Gros et al in patients with metastatic melanoma.[17] They speculated that HLA-DR expression on MDSCs distinguishes suppressive from nonsuppressive T-cells. However, our preliminary experiments with anti-HLA blocking monoclonal antibodies did not lead to different results, suggesting that HLA-DR expression is not a decisive factor. As we demonstrate that tumor-derived MDSCs express significant amount of arginase I, our findings do not rule out that tumor-derived MDSCs are able to suppress T-cell functions in vivo, because our T-cell suppression assay with a co-culture time of more than 96 hours might not reflect the immediate suppressive capacity of tumor-derived MDSCs. Moreover, tumor-specific co-factors that are essential for the release of arginase I-containing granules from tumor-derived MDSCs into the culture supernatant might also be lacking.[8,18]

Considering that tumor-derived MDSCs upregulate HLA-DR and thus might act as antigen-presenting cells, we wondered whether there was a relationship between different MDSCs and CD4$^+$ T-cell subsets at the tumor site. Correlation analysis revealed that the frequency of granulocytic MDSCs correlated positively with the frequency of CD4$^+$ $T_{EM}$. CD4$^+$ $T_{EM}$ proved to be the predominant CD4$^+$ T-cell subset inside the tumor, suggesting that $T_{EM}$ are particularly capable of infiltrating glioma tissue. Similar observations with preferential accumulation of $T_{EM}$ have been made in other tumor entities including renal cell carcinoma and breast cancer.[19,20] Further analysis revealed that GBM-infiltrating CD4$^+$ $T_{EM}$ strongly upregulate PD-1, an immunoinhibitory receptor that is expressed by chronically activated T-cells and involved in functional T-cell exhaustion.[21,22] Consistent with these observations, PD-1 expression was inversely correlated with the ability of CD4$^+$ tumor-infiltrating $T_{EM}$ to produce INF-γ. Moreover, tumor-infiltrating CD4$^+$ $T_{EM}$ also expressed HLA-DR and downregulated CD127, a typical expression profile of exhausted T-cells.[23–25]

To provide more evidence for an association of tumor-derived granulocytic MDSCs with CD4$^+$ $T_{EM}$, we also analyzed PD-L1 expression on different MDSC subsets. Glioma-related PD-L1 has been previously identified as a strong inhibitor of CD4$^+$ T-cell activation as assessed by increased INF-γ production in the presence of neutralizing antibodies.[26] We found that only a minority of MDSCs, mainly monocytic MDSCs, in peripheral blood expressed PD-L1. In contrast, PD-L1 expression was significantly upregulated in tumor-derived MDSCs with higher frequencies in the monocytic MDSC fraction. This observation is supported by a previous report from Bloch et al, who showed that circulating monocytes and glioma-associated macrophages can upregulate PD-L1 expression via autocrine/paracrine IL-10 production.[27] Hypoxic conditions with increased expression of HIF-1α within GBMs might also favor PD-L1 upregulation on MDSCs.[28] Ultimately, we demonstrated that PD-1 upregulation on CD4$^+$ $T_{EM}$ can be induced by freshly prepared tumor-derived MDSCs, further supporting their potential role in driving T-cell exhaustion inside the tumor. Further studies are necessary to evaluate whether glioma-derived MDSCs can induce antigen-specific CD4$^+$ tolerance or T-cell exhaustion, as has been shown for MHC class-II expressing MDSCs in a mouse tumor model.[29] To get more insight into the regulation of antigen-specific CD4$^+$ $T_{EM}$ exhaustion in GBMs, it would be interesting to study the interaction between tumor-infiltrating MDSCs and CD4$^+$ $T_{EM}$ in GBM patients who are vaccinated with glioma-specific peptides such as EGFRvIII targeted peptides.[30]

We believe that the results of our study have important clinical implications for immune-based interventions in GBMs. Firstly, granulocytic MDSCs in peripheral blood and tumor tissue should be carefully monitored during immunotherapeutic studies in GBM patients. Secondly, strategies to target MDSCs in peripheral blood and tumor tissue should be implemented into immunotherapeutic approaches. Thirdly, the finding that PD-1 was strongly upregulated in CD4$^+$ $T_{EM}$ within tumor tissue and PD-L1 is expressed in tumor-derived MDSCs, provides a rationale for the treatment of GBMs with PD-1 antagonists to

block intratumoral exhaustion of $CD4^+$ $T_{EM}$ and to restore their function.[31] Strategies to prevent $CD4^+$ $T_{EM}$ exhaustion will be essential for building effective antitumor immunity within GBMs because tumor-specific $CD4^+$ T-cells can enhance CD8 T-cell recruitment and CD8-mediated tumor rejection of GBMs.[32]

## Supplementary material

Supplementary material is available online at *Neuro-Oncology* (http://neuro-oncology.oxfordjournals.org/).

## Funding

This study was funded in part by the Wilhelm-Sander-Foundation (Grant 2009.804.1 to O.M.G and U.B).

## Acknowledgments

We would like to thank Verena Schütte and Barbara Wrobel for their excellent technical assistance. We would also like to thank C. Ewelt, M. Holling, and N. Warneke for the acquisition of tumor tissue.

*Conflict of interest statement*. None declared.

## References

1. Nagaraj S, Gabrilovich DI. Myeloid-derived suppressor cells in human cancer. *Cancer J*. 2010;16(4):348–353.
2. Condamine T, Gabrilovich DI. Molecular mechanisms regulating myeloid-derived suppressor cell differentiation and function. *Trends Immunol*. 2011;32(1):19–25.
3. Rodrigues JC, Gonzalez GC, Zhang L, et al. Normal human monocytes exposed to glioma cells acquire myeloid-derived suppressor cell-like properties. *Neuro Oncol*. 2010;12(4):351–365.
4. Solito S, Marigo I, Pinton L, Damuzzo V, Mandruzzato S, Bronte V. Myeloid-derived suppressor cell heterogeneity in human cancers. *Ann N Y Acad Sci*. 2014;1319:47–65.
5. Gabrilovich DI, Nagaraj S. Myeloid-derived suppressor cells as regulators of the immune system. *Nat Rev Immunol*. 2009;9(3):162–174.
6. Peranzoni E, Zilio S, Marigo I, et al. Myeloid-derived suppressor cell heterogeneity and subset definition. *Curr Opin Immunol*. 2010;22(2):238–244.
7. Raychaudhuri B, Rayman P, Ireland J, et al. Myeloid-derived suppressor cell accumulation and function in patients with newly diagnosed glioblastoma. *Neuro Oncol*. 2011;13(6):591–599.
8. Sippel TR, White J, Nag K, et al. Neutrophil degranulation and immunosuppression in patients with GBM: restoration of cellular immune function by targeting arginase I. *Clin Cancer Res*. 2011;17(22):6992–7002.
9. Felsberg J, Rapp M, Loeser S, et al. Prognostic significance of molecular markers and extent of resection in primary glioblastoma patients. *Clin Cancer Res*. 2009;15(21):6683–6693.
10. Schroeteler J, Reeker R, Suero Molina E, et al. Glioma tissue obtained by modern ultrasonic aspiration with a simple sterile suction trap for primary cell culture and pathological evaluation. *Eur Surg Res*. 2014;53(1–4):37–42.
11. Grauer OM, Nierkens S, Bennink E, et al. CD4+FoxP3+ regulatory T-cells gradually accumulate in gliomas during tumor growth and efficiently suppress antiglioma immune responses in vivo. *Int J Cancer*. 2007;121(1):95–105.
12. Jacobs JF, Idema AJ, Bol KF, et al. Regulatory T-cells and the PD-L1/PD-1 pathway mediate immune suppression in malignant human brain tumors. *Neuro Oncol*. 2009;11(4):394–402.
13. Gielen PR, Schulte BM, Kers-Rebel ED, et al. Increase in both CD14-positive and CD15-positive myeloid-derived suppressor cell subpopulations in the blood of patients with glioma but predominance of CD15-positive myeloid-derived suppressor cells in glioma tissue. *J Neuropathol Exp Neurol*. 2015;74(5):390–400.
14. Raychaudhuri B, Rayman P, Huang P, et al. Myeloid derived suppressor cell infiltration of murine and human gliomas is associated with reduction of tumor infiltrating lymphocytes. *J Neurooncol*. 2015;122(2):293–301.
15. Umemura N, Saio M, Suwa T, et al. Tumor-infiltrating myeloid-derived suppressor cells are pleiotropic-inflamed monocytes/macrophages that bear M1- and M2-type characteristics. *J Leukoc Biol*. 2008;83(5):1136–1144.
16. Kohanbash G, McKaveney K, Sakaki M, et al. GM-CSF promotes the immunosuppressive activity of glioma-infiltrating myeloid cells through interleukin-4 receptor-alpha. *Cancer Res*. 2013;73(21):6413–6423.
17. Gros A, Turcotte S, Wunderlich JR, Ahmadzadeh M, Dudley ME, Rosenberg SA. Myeloid cells obtained from the blood but not from the tumor can suppress T-cell proliferation in patients with melanoma. *Clin Cancer Res*. 2012;18(19):5212–5223.
18. Haverkamp JM, Crist SA, Elzey BD, Cimen C, Ratliff TL. In vivo suppressive function of myeloid-derived suppressor cells is limited to the inflammatory site. *Eur J Immunol*. 2011;41(3):749–759.
19. Beckhove P, Feuerer M, Dolenc M, et al. Specifically activated memory T-cell subsets from cancer patients recognize and reject xenotransplanted autologous tumors. *J Clin Invest*. 2004;114(1):67–76.
20. Attig S, Hennenlotter J, Pawelec G, et al. Simultaneous infiltration of polyfunctional effector and suppressor T-cells into renal cell carcinomas. *Cancer Res*. 2009;69(21):8412–8419.
21. Wherry EJ. T-cell exhaustion. *Nat Immunol*. 2011;12(6):492–499.
22. Day CL, Kaufmann DE, Kiepiela P, et al. PD-1 expression on HIV-specific T-cells is associated with T-cell exhaustion and disease progression. *Nature*. 2006;443(7109):350–354.
23. Lang KS, Recher M, Navarini AA, et al. Inverse correlation between IL-7 receptor expression and CD8 T-cell exhaustion during persistent antigen stimulation. *Eur J Immunol*. 2005;35(3):738–745.
24. Thompson RH, Dong H, Lohse CM, et al. PD-1 is expressed by tumor-infiltrating immune cells and is associated with poor outcome for patients with renal cell carcinoma. *Clin Cancer Res*. 2007;13(6):1757–1761.
25. Ahmadzadeh M, Johnson LA, Heemskerk B, et al. Tumor antigen-specific CD8 T-cells infiltrating the tumor express high levels of PD-1 and are functionally impaired. *Blood*. 2009;114(8):1537–1544.
26. Wintterle S, Schreiner B, Mitsdoerffer M, et al. Expression of the B7-related molecule B7-H1 by glioma cells: a potential mechanism of immune paralysis. *Cancer Res*. 2003;63(21):7462–7467.

27. Bloch O, Crane CA, Kaur R, Safaee M, Rutkowski MJ, Parsa AT. Gliomas promote immunosuppression through induction of B7-H1 expression in tumor-associated macrophages. *Clin Cancer Res*. 2013;19(12):3165–3175.
28. Noman MZ, Desantis G, Janji B, et al. PD-L1 is a novel direct target of HIF-1alpha, and its blockade under hypoxia enhanced MDSC-mediated T-cell activation. *J Exp Med*. 2014;211(5):781–790.
29. Nagaraj S, Nelson A, Youn JI, Cheng P, Quiceno D, Gabrilovich DI. Antigen-specific CD4(+) T-cells regulate function of myeloid-derived suppressor cells in cancer via retrograde MHC class II signaling. *Cancer Res*. 2012;72(4):928–938.
30. Schuster J, Lai RK, Recht LD, et al. A phase II, multicenter trial of rindopepimut (CDX-110) in newly diagnosed glioblastoma: the ACT III study. *Neuro Oncol*. 2015;17(6):854–861.
31. Lei GS, Zhang C, Lee CH. Myeloid-derived suppressor cells impair alveolar macrophages through PD-1 receptor ligation during Pneumocystis pneumonia. *Infect Immun*. 2015;83(2):572–582.
32. Hoepner S, Loh JM, Riccadonna C, et al. Synergy between CD8 T-cells and Th1 or Th2 polarised CD4 T-cells for adoptive immunotherapy of brain tumours. *PLoS One*. 2013;8(5):e63933.